

Tethered Diblock Copolymer Chains on Platelets Prepared by Semicrystalline ABC Triblock Copolymers in Toluene with Trace Amounts of Water

Weihuan Huang, Chunxia Luo, Jilin Zhang, Kai Yu, and Yanchun Han*

State Key Laboratory of Polymer Physics and Chemistry, Changchun Institute of Applied Chemistry, Graduate University of the Chinese Academy of Sciences, Chinese Academy of Sciences, 5625 Renmin Street, Changchun 130022, People's Republic of China

Received April 20, 2007; Revised Manuscript Received August 10, 2007

ABSTRACT: Lamellar platelets of triblock copolymers grown in dilute toluene solution with trace amounts of water can be used as templates for tethered diblock copolymer chain preparation and analysis. Polystyrene-*b*-poly(2-vinylpyridine)-*b*-poly(ethylene oxide) (PS-*b*-P2VP-*b*-PEO) with two different block fractions were used as model templates to generate tethered P2VP-*b*-PS chains on the platelet basal surfaces. In toluene solution the aggregation states of PS-*b*-P2VP-*b*-PEO were sensitive to the water content in the solution. For toluene with trace amount of water, spherical micelles were formed in the early stage and large square platelets would gradually grow from these spherical micelles. The hydrogen bonding between water and EO units was responsible for the formation of micelles and subsequent square platelets in the solution. Tethered P2VP-*b*-PS chains on basal surface of PEO platelets could be regarded as diblock copolymer brushes and the density (σ : 0.086–0.36) and height (d : 3.5–14.3 nm) of these tethered chains could be easily modulated by changing the crystallization condition and/or the molecular weight of each block. The tethered P2VP-*b*-PS chains were responsive to different solvent vapor. The selectivity of tethered blocks to various solvents is responsible for the change of morphologies of the basal surface of the platelets.

Introduction

Polymer brushes refer to an assembly of polymer chains tethered by one end to a surface or interface.¹ Theoretical studies indicated that many factors, such as grafting density, molecular weight, chemical composition, solvents, and temperature, can influence behaviors of tethered block copolymer brushes.^{2–6} For tethered linear flexible AB diblock copolymer brushes, patterned films could form in a selective solvent in which the polymer–solvent interactions for each block are different.⁷ The responsive properties can be exploited in the development of “smart” surface and nanoactuators.^{1,5}

Polymer brushes are typically synthesized by physisorption and covalent attachment. Covalent attachment of polymer brushes are normally prepared by either “grafting to”⁸ or “grafting from”⁹ techniques. In order to achieve uniform tethering density and narrow molecular weight distribution of the tethered chains, crystalline–amorphous block copolymers can be used to grow platelets in dilute solutions, which have a “sandwiched” structure with the single crystal in the middle covered by two nanoamorphous block layers on the top and bottom of the basal surface of platelets.^{10–15} Cheng et al. have designed an experiment to detect the interaction changes of the tethered homopolymer polystyrene (PS) chains on the poly(ethylene oxide) (PEO) or poly(L-lactic acid) (PLLA) platelet basal surfaces using PEO-*b*-PS or PEO-*b*-PLLA diblock copolymer.^{12,13} They also created tethered diblock copolymer poly(methyl methacrylate)-*b*-polystyrene (PMMA-*b*-PS) on the basal surface of PLLA platelets using self-seeding technique of triblock copolymer PMMA-*b*-PS-*b*-PLLA.¹⁴

Self-seeding technique is based on partly dissolving pre-formed crystals at lower crystallization temperature. The sample

is subsequently reheating to a seeding temperature and then quickly cooled to a preset crystallization temperature to grow single crystals. Continuation of the procedure to higher temperature dissolves most of the crystals, leaving microscopic nuclei to grow a uniformly sized population of crystals. So the self-seeding technique is probably now the most widely used method of growing polymer lamellae from dilute solution.^{11,16–18} The morphology of polymer single crystals critically depends on the crystallization conditions, such as solution concentration, crystallization temperature, self-seeding temperature, etc. The main drawback of self-seeding method is that the precise control of different temperatures is necessary to the success of this technique. Herein, we developed a novel and simple approach to prepared platelets with uniform and controllable size via modulation of the water content in the solution. We produced lamellar platelets of a semicrystalline ABC triblock copolymer, polystyrene-*b*-poly(2-vinylpyridine)-*b*-poly(ethylene oxide) (PS-*b*-P2VP-*b*-PEO), in toluene with trace amounts of water. The obtained lamellar platelets can act as templates for tethered P2VP-*b*-PS diblock chain analysis. This embodies one of the advantages of triblock copolymers over diblock copolymers.^{19–26} We found that the trace amount of water in the solution could greatly influence the solubility and aggregation behavior of PEO blocks in toluene. We studied the influence of water content in solution on the structure of obtained platelets and the unique morphological evolution from spherical micelles to square platelets in the solution. The tethered P2VP-*b*-PS chains on the basal surface of PEO platelets had similar behavior with normal block brushes on flat substrate when they were exposed to different solvent vapor because of the selectivity of tethered blocks to various solvents. The surface morphology of these tethered block copolymer brushes can be reversibly changed under the treatment of different solvent vapor.

* Corresponding author. Telephone: 86-431-85262175. Fax: 86-431-85262126. E-mail: ychan@ciac.jl.cn.

Table 1. Molecular Weight of Each Block and Polydispersity of Two Series of PS-*b*-P2VP-*b*-PEO Triblock Copolymers

sample	$M_n(\text{PS})$	$M_n(\text{P2VP})$	$M_n(\text{PEO})$	$M_w/M(\text{copolymer})$
1# PS- <i>b</i> -P2VP- <i>b</i> -PEO (14.1–12.3–35.0)	14 100	12 300	35 000	1.08
2# PS- <i>b</i> -P2VP- <i>b</i> -PEO (20.1–14.2–26.0)	20 100	14 200	26 000	1.10

Experimental Section

Sample Preparation. Two polystyrene-*b*-poly(2-vinylpyridine)-*b*-poly(ethylene oxide) (PS-*b*-P2VP-*b*-PEO) copolymers were supplied by Polymer Source, Inc. The characteristics of these two copolymers are summarized in Table 1, according to the data of the provider. The solvent, toluene, purchased from the Alfa Inc. and the Beijing Chemical Plant were found to produce identical results. The PS-*b*-P2VP-*b*-PEO copolymers were dissolved in (i) toluene dried with MgSO_4 , (ii) distilled toluene, (iii) toluene without any treatment, and (iv) toluene with additional water. In some case, as indicated in the context, magnetic stirring for 3 days was performed before storage at room temperature for various periods. In other case, PS-*b*-P2VP-*b*-PEO was dissolved in toluene by heating the solution to 40–60 °C for ca. 5 min.²⁷ The concentration of PS-*b*-P2VP-*b*-PEO was 0.1 wt % or 0.2 wt %. The PS-*b*-P2VP-*b*-PEO thin films were prepared by spin-coating the dilute solution onto the freshly cleaved mica at 2500 rpm for 90 s. Spin-coating was performed on a commercial spin-coater KW-4A, Chemat Technology Inc.

Treatment of Tethered P2VP-*b*-PS Chains with Different Solvent Vapor. The tethered P2VP-*b*-PS chains on the basal surfaces of platelets grown in distilled toluene were exposed to saturated ethanol, 1,4-dioxane, or toluene vapor in closed vessels for 60 min at room temperature. The samples were then removed from the solvent vapor and dried in air for at least 60 min before any further characterization.

Characterization. The morphologies of crystals or aggregates of PS-*b*-P2VP-*b*-PEO in toluene were investigated by atomic force microscopy (AFM) and transmission electron microscopy (TEM). AFM images were acquired (SPA300HV/SPI3800N Probe Station, Seiko Instruments Inc., Japan) in tapping mode. A silicon microcantilever (spring constant 2 N/m and resonance frequency ~70 kHz, Olympus Co., Japan) with an etched conical tip (radius of curvature ~40 nm as characterized by scanning over very sharp needle array (NT-MDT, Russia)) was used for scan. TEM experiments were carried out on a JEM-1011 transmission electron microscope (JEOL Inc., Japan) operated at 100 kV accelerating voltage. The samples for TEM were prepared by dipping a drop of copolymer solution on a copper grid and wicking away the excess solution with filter paper. Surface enhanced Raman scattering (SERS) spectra were measured with a Renishaw 2000 Raman spectrometer (Renishaw Ltd., Gloucestershire, United Kingdom). Radiation of 514 nm from an air-cooled argon ion laser was used for the SERS excitation with power of not more than a few milliwatts at the sample position. The silver mirror was prepared by dipping a clean glass plate into a solution of silver ammonia complex and acetaldehyde. The glass plate was washed with distilled water and then, dried under high vacuum overnight. The lamellar platelets were spin-coated onto the glass platelets at 2500 rpm for 90 s. The glass platelets were then dried under high vacuum and were ready for further measurements. In order to identify the FT-SERS spectra of tethered diblock copolymers, we also carried out the SERS experiments on P2VP and PS homopolymers. The strong peaks at 1123 cm^{-1} in all spectra were caused by the daylight.

Results and Discussion

A. Preparation of Platelets from Toluene with Trace Amount of Water. 1. Effect of the Water to EO Molar Ratio (Z) on Morphology of Aggregates. Figure 1 shows different crystals or aggregates of 1# PS-*b*-P2VP-*b*-PEO (14.1–12.3–35.0) formed in various mixtures of toluene and water. The molar ratio of water and EO unit in the solution played an important role in the aggregation behavior of PS-*b*-P2VP-*b*-PEO. When the concentration of PS-*b*-P2VP-*b*-PEO was 0.1

wt % in toluene dried with MgSO_4 ($Z \approx 0$), a few multilayer crystals could be observed on the spin-coated film (Figure 1a). The sizes of these multilayer crystals were polydispersed (from the results of light microscope), and the average value was about 8 μm . When the concentration of PS-*b*-P2VP-*b*-PEO was 0.2 wt % in toluene without any treatment ($Z \approx 0.75$, the water concentration in untreated toluene is about 0.03 vol %), a small quantity of multilayer or monolayer crystals could be obtained (Figure 1b). The sizes of these crystals were uniform (about 5 μm) although they were not perfect platelets. When the concentration of PS-*b*-P2VP-*b*-PEO was 0.1 wt % in distilled toluene ($Z \approx 0$ –1.5), regular square platelets with monodispersed size of 2 μm could be routinely observed on the spin-coated film or slowly dried film on copper grid (Figure 1c). These platelets were identical with those observed in PEO homopolymer¹⁷ or PS-*b*-PEO copolymer^{11,16} platelets and the selective area electron diffraction (SAED) pattern (inset of Figure 1c') was recognized to be the [001] zone pattern of the monoclinic lattice of PEO,^{16,17} indicating that the chain directions in both "sandwiched" crystals were parallel to their lamellar surface normal. All other square platelets of two PS-*b*-P2VP-*b*-PEO grown at different conditions had similar TEM images and SAED patterns. When the concentration of PS-*b*-P2VP-*b*-PEO was 0.1 wt % in toluene without any treatment ($Z \approx 1.5$), small platelets with monodispersed size of 0.2 μm could be obtained (Figure 1d). When the concentration of PS-*b*-P2VP-*b*-PEO was 0.04 wt % in toluene without any treatment ($Z \approx 3.8$), square platelets and spherical micelles could be simultaneously observed (Figure 1e). Further increase of content of water resulted in the disappearance of platelets and formation of a few irregular aggregates (not shown).

2. Evolution from Micelles to Square Platelets. Figure 2 shows the evolution of aggregates of 1# PS-*b*-P2VP-*b*-PEO (14.1–12.3–35.0) (0.1 wt % in toluene without any treatment, $Z \approx 1.5$) with aging time. The stock solution was stirred for 3 days and then aged at room temperature for various periods. When the solution was aged for 3 days after stirring, most micelles were spheres with the diameter of about 50 nm (Figure 2a). After this was aged at room temperature for 109 days, some quasi-rectangular aggregates with the size of 60–180 nm could be observed (Figure 2b). When the solutions were aged for even longer times (115 days), many quasi-square aggregates with the size of about 500 nm could be routinely obtained (Figure 2c). After this was aged for 169 days, more regular square platelets with the size of about 200 nm could be observed (Figure 2d). The difference of the size of the aggregates in parts c and d of Figure 2 may partially produced by the sample preparation procedure and the amplification effect of the AFM tip. The nuclei could be clearly seen in the center of the platelets from both the AFM and TEM images.

3. Mechanism for Aggregation Behavior of PS-*b*-P2VP-*b*-PEO in Toluene with Various Amounts of Water. The self-assembly of block copolymers in organic solvents can be modulated by the water content in the solution. Jérôme et al. reported the different aggregation behaviors of PS-*b*-P2VP-*b*-PEO in water/toluene mixtures with various composition.²⁸ The self-organization of the PS-*b*-P2VP-*b*-PEO at the water/toluene interface of the water-in-toluene and toluene-in-water emulsions was responsible for the different structures of the formed

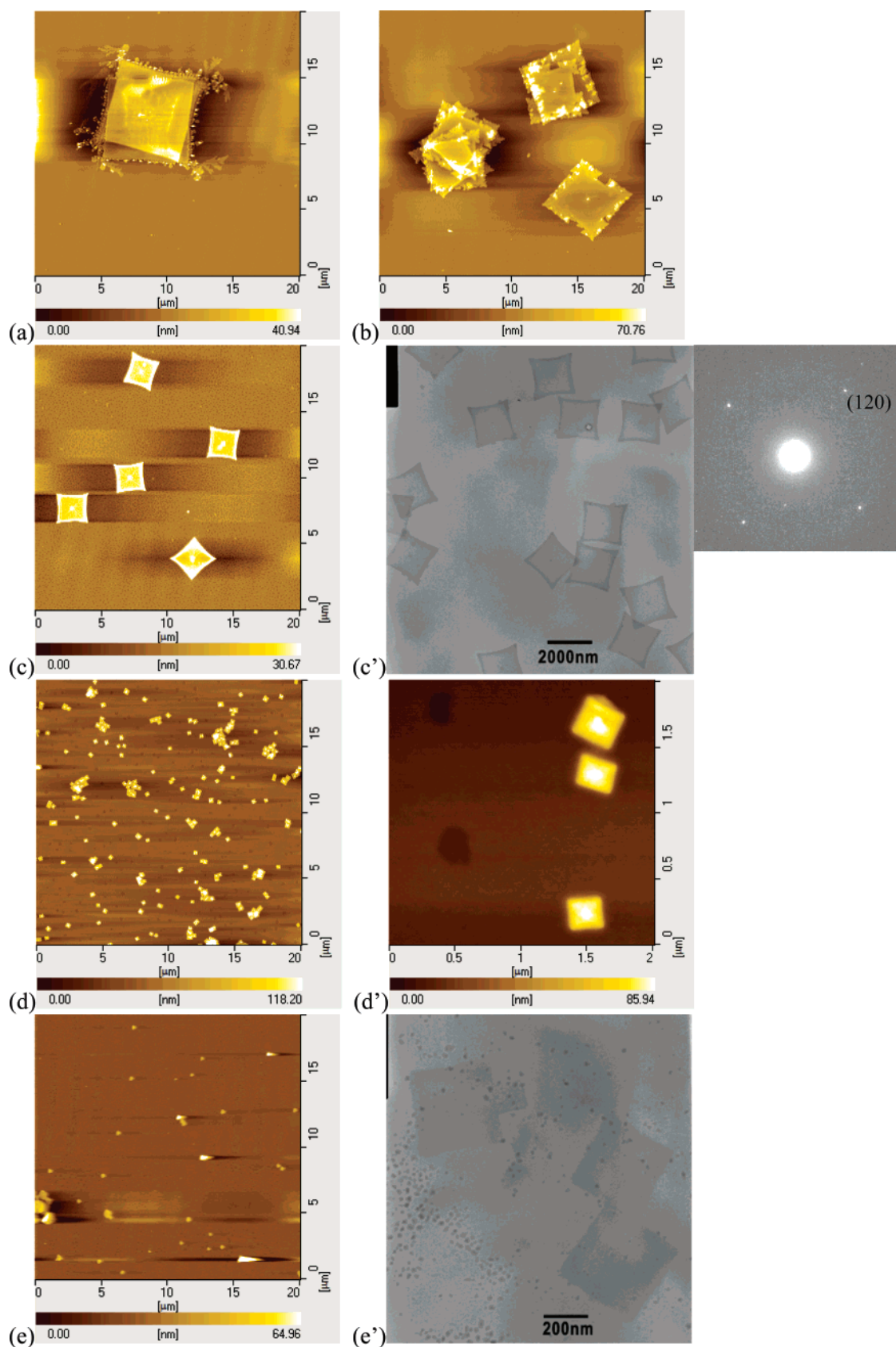


Figure 1. AFM height images and TEM images (c' and d') of aggregates formed in solution with various molar ratio of water to EO unit (Z): (a) ~ 0 , (b) 0.75, (c) ~ 0 –1.5, (d) 1.5, and (e) 3.8. Inset of part c' shows the selective area electron diffraction (SAED) pattern.

aggregates. In fact, the compatibility of water and EO units also determined the aggregation behaviors of other systems, such as PS–PEO in cyclopentane,^{29–31} Pluronic L64 in *o*-xylene,^{32,33} and Pluronic L92 in *p*-xylene.³⁴ However, few investigations have been reported about the transformation of the micelles to

regular platelets, especially for semicrystalline ABC triblock copolymers. As discussed in ref 28, when PS-*b*-P2VP-*b*-PEO was dissolved in pure toluene, no micellization occurred. Nevertheless trace amounts of water in the solution could result in the aggregation of the triblock copolymer. Similar effect of

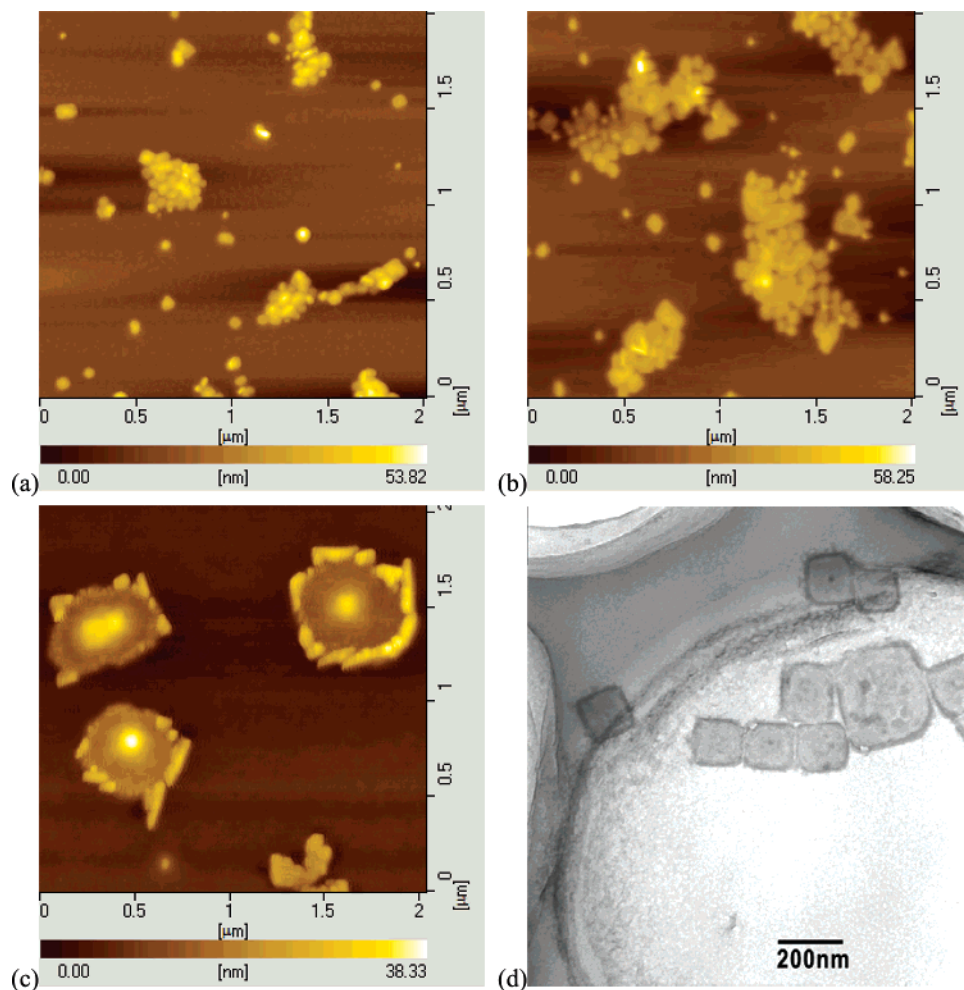


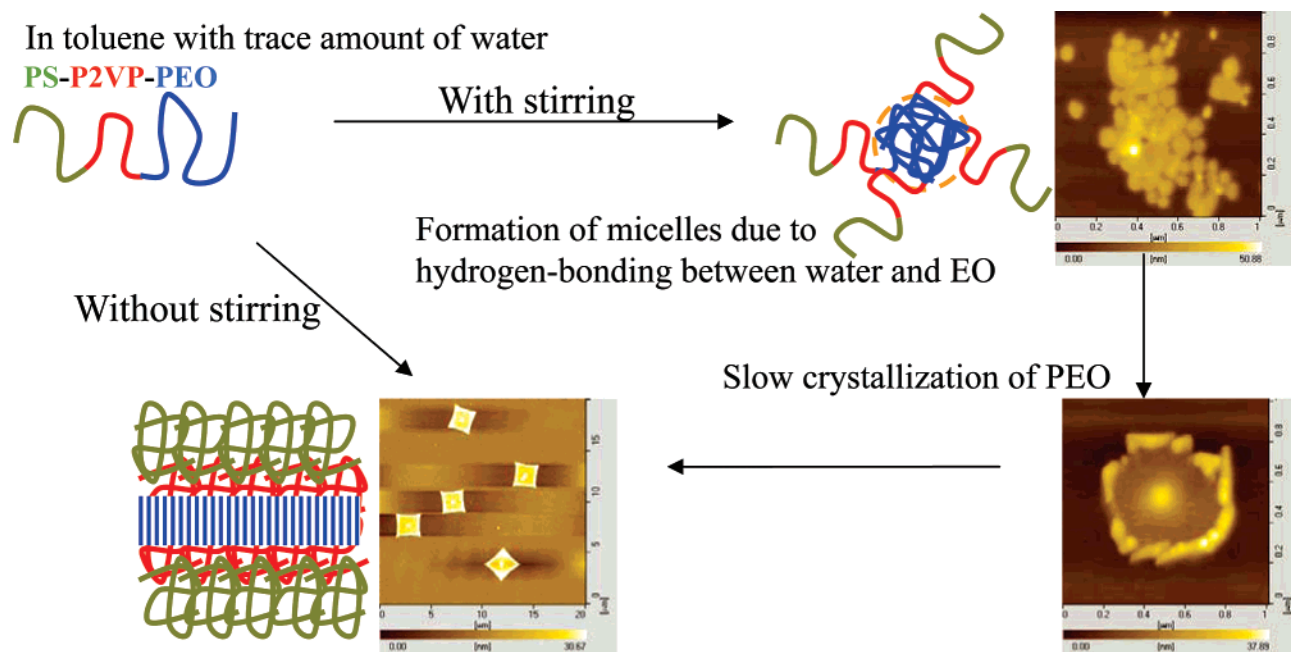
Figure 2. AFM images (a–c) and TEM image (d) of aggregates (formed from 1# PS-*b*-P2VP-*b*-PEO 0.1 wt % in toluene without any treatment, $Z \approx 1.5$) after stirring for 3 days and then aged at room temperature for various periods: (a) 3 days, (b) 109 days, (c) 115 days, and (d) 169 days.

water on the self-assembly of PEO containing copolymers had been reported. The primary role of water is to solvate the PEO blocks by hydrogen bonding and the water to EO molar ratio (Z) played an important role in determining the structure of aggregates in the solution.^{28–35} The limit of solubility of water in toluene at room temperature was ~ 0.03 vol %.²⁸ Then for 1# PS-*b*-P2VP-*b*-PEO (14.1–12.3–35.0) 0.1 wt % in toluene without any treatment, Z was about 1.5. Spherical micelles consisting of a hydrated PEO core, a P2VP shell and a PS corona²⁸ were obtained by stirring the solution for 3 days. The shape of micelles in the mixed solvent is the result of the minimum of the thermodynamic equilibrium, which can be calculated using the concept of reduced tethering density in micelle system.^{36,37} Due to the crystallization of core forming blocks (PEO), these micelles were not stable.^{38–45} When the solution was stored at room temperature without stirring for a long period, spherical micelles would gradually evolve to square platelets (Scheme 1). Since the crystallizable blocks were isolated in each core of the spherical micelle, the growth of square platelets was a quite slow process (about 6 months, Figure 2).⁴⁶

On the other hand, when the stock solution was not stirred before the storage at room temperature, formation of regular square platelets could be completed in relative short period (about 1 month). This can be explained by the heterogeneous nucleation due to incomplete dissolution on a microscopic order without stirring.⁴⁷ The crystallization behavior of PEO homopolymer or block copolymers has been widely investigated.^{10,48–55}

Amis et al. found that no crystallization of PEO in pure toluene occurred when the solution were held at 20 °C for several days. Clusters consisted of several staggered layers developed after an aliquot of seed suspension was added to the very dilute PEO solution of toluene.⁵⁶ Branched layers of lamellae of PEO could grow in more concentrated solution of toluene.⁴⁷ Gast et al. investigated the competition between spherical micelles and semicrystalline aggregates of PS-*b*-PEO in cyclopentane, a selective solvent for PS blocks.³¹ This is similar to our results because the hydration of PEO and toluene makes PEO seemingly insoluble in toluene, although pure toluene is a good solvent for dried PEO.³⁵ Then the hydrogen bonding between the water and EO facilitated the nucleation of the crystallization of PEO blocks in toluene with trace amounts of water. So it is reasonable that the size and structure of the crystals depended on the Z values (Figure 1). When toluene was dried with MgSO_4 , the amount of water in the solution was quite small. The obtained crystals were multilayer, and the total number of these crystals was very few probably due to the rare nuclei in the solution (Figure 1a). When distilled toluene was used to dissolve PS-*b*-P2VP-*b*-PEO copolymers, the size of the platelets decreased and the number increased since the water in the distilled toluene was more than that in the toluene dried with MgSO_4 (Figure 1c). The water content in the toluene without any treatment further increased and the size and number of the platelets further decreased and increased, respectively (Figure 1d). For 1# PS-*b*-P2VP-*b*-PEO (14.1–12.3–35.0) 0.04, 0.1, and 0.2 wt % in toluene without any treatment, Z values were about

Scheme 1. Schematic Representation of the Morphological Evolution of PS-*b*-P2VP-*b*-PEO in Toluene with Trace Amounts of Water with or without Stirring



3.8, 1.5, and 0.75, respectively. So the size and number of crystals in 0.2 wt % toluene without any treatment were larger and smaller than that of 0.1 wt % solution, respectively (Figure 1b). When the concentration of 1# PS-*b*-P2VP-*b*-PEO (14.1–12.3–35.0) in toluene without any treatment was 0.04 wt %, all the hydrogen-bonding sites of the PEO blocks were saturated by water, which produced many spherical micelles at the expense of the disappearance of some platelets (Figure 1e).

B. Properties of Tethered Diblock Copolymer Chains on Platelets. 1. Structure of Tethered P2VP-*b*-PS Chain. Like the crystalline–amorphous diblock copolymers, PS-*b*-P2VP-*b*-PEO triblock copolymers also grow the platelets having a “sandwiched” structure with the PEO single crystals in the middle covered by the two amorphous layers on the top and bottom of the PEO basal surface, respectively. Then the P2VP-*b*-PS blocks can be viewed as the tethered chains on a substrate. Cheng et al. have developed an approach to study the interactions of the tethered PS chains on the PEO or PLA single-crystal basal surface with controlled and uniform tethering densities.^{12,13} In this paper, we adopt a similar method to analyze the properties of the tethered diblock chains on the basal surface of PEO platelets. An overall thickness of a semicrystalline block copolymer platelet (d_{overall}) after drying can be measured using atomic force microscopy (AFM). To calculate the thickness of crystals (d_{PEO}) and the thickness of the tethered amorphous chains (d_a) values based on the d_{overall} (Scheme 2), we modify the approximations developed by Cheng et al.^{12,13} as follows:

$$d_{\text{PEO}} = d_{\text{overall}} v_{\text{PEO}}$$

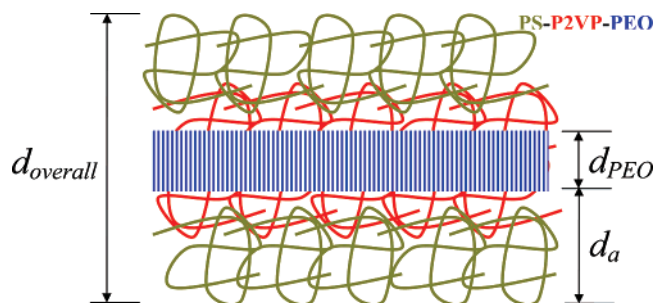
and

$$v_{\text{PEO}} = \frac{M_n^{\text{PEO}}/\rho_{\text{PEO}}}{M_n^{\text{PEO}}/\rho_{\text{PEO}} + M_n^{\text{P2VP}}/\rho_{\text{P2VP}} + M_n^{\text{PS}}/\rho_{\text{PS}}} \quad (1a)$$

$$d_a = \frac{d_{\text{overall}} - d_{\text{PEO}}}{2} \quad (1b)$$

where M_n^{PEO} , M_n^{P2VP} , and M_n^{PS} are the MW's of the PEO, P2VP,

Scheme 2. Schematic Representation of the Multilayered Structure of Tethered P2VP-*b*-PS Diblock Brush on Basal Surfaces of PEO Platelets



and PS blocks, ρ_{PEO} , ρ_{P2VP} , and ρ_{PS} are densities of the corresponding blocks, and v_{PEO} represents the volume fraction of PEO blocks, respectively. According to the results of Cheng et al., the crystallinity of PEO in the platelets is about 95% and thus the practical density of the PEO crystals is about 1.23 g/cm³.^{11–13} For a semicrystalline block copolymer, the density of the tethered amorphous blocks on the platelet surface of the crystalline blocks, σ , can be calculated by¹³

$$\sigma = 1/\left(\frac{2M_n^{\text{PEO}}}{N_A \rho_{\text{PEO}} d_{\text{PEO}}}\right) = \frac{N_A \rho_{\text{PEO}} d_{\text{PEO}}}{2M_n^{\text{PEO}}} \quad (2)$$

where N_A is Avogadro's number. The thickness of platelets could be modulated by changing the condition of crystallization, such as the concentration of PS-*b*-P2VP-*b*-PEO and water. The calculated values about these platelets grown in different condition are summarized in Table 2. The tethering densities can be varied from very low (0.086) to quite high (0.36). The total thickness of the platelets is in inverse proportion to the size for the platelets of the same triblock copolymer grown in toluene with various amounts of water. In other words, high tethering density and height can be obtained with large water to EO molar ratio. For the platelets of triblock copolymers with different molecular weight of each block grown under the same condition, the total thickness of 1# PS-*b*-P2VP-*b*-PEO (14.1–

Table 2. List of Calculated Tethering Heights and Densities of P2VP-*b*-PS Diblock Brush on Basal Surfaces of PEO Platelets Grown under Various Conditions

	PS- <i>b</i> -P2VP- <i>b</i> -PEO (14.1–12.3–35.0)			PS- <i>b</i> -P2VP- <i>b</i> -PEO (20.1–14.2–26.0)
ν_{PEO}	0.54			0.40
d_{overall} (nm)	62.0 ^a	15.0 ^b	18.0 ^c	42.0 ^a
d_{PEO} (nm)	33.5	8.1	9.7	16.8
d_a (nm)	14.3	3.5	4.2	12.6
σ	0.36	0.086	0.10	0.24

^a 0.1 wt % in toluene without any treatment ($Z \approx 1.5$). ^b 0.2 wt % in toluene without any treatment ($Z \approx 0.75$). ^c 0.1 wt % in distilled toluene ($Z \approx 0-1.5$).

12.3–35.0) is larger than that of 2# PS-*b*-P2VP-*b*-PEO (20.1–14.2–26.0) probably due to the higher PEO fraction and molecular weight of the former triblock copolymer (Table 2).

2. Response of Tethered P2VP-*b*-PS Chain to Different Solvents. We choose the platelets of 1# PS-*b*-P2VP-*b*-PEO (14.1–12.3–35.0) grown in the distilled toluene to investigate the response of the tethered P2VP-*b*-PEO chains to different solvents because of their regularity and large size (Figure 1c), compared with platelets grown under other conditions. We should emphasize that the glass transition temperature is suppressed more than the melt temperature when the polymers are exposed to solvent or solvent vapor because the solvent molecules cannot easily diffuse in the compactly folding chains. So the structure of the PEO crystals will not undergo significant change after treated in various solvent vapors. We utilized surface enhanced Raman scattering (SERS) to determine the surface chemistry of the PEO lamellar platelets before and after different solvent vapor treatments (Figure 3). The spectra of homopolymer P2VP and PS were measured as the reference (Figure 3b). The bottom spectrum of Figure 3a was obtained from platelets grown in toluene solution. It showed two characteristic vibrations associated with PS, one at 1617 cm^{-1} ($\nu(8a)$ of PS)⁵⁷ and one at 1002 cm^{-1} (“breathing” mode of benzene rings) [14b]. The middle spectrum of Figure 3a was obtained after treatment with 1,4-dioxane (common solvent for PS and P2VP blocks) vapor for 1 h. It showed another characteristic vibration associated with PS, at 1597 cm^{-1} ($\nu(8b)$ of PS).⁵⁷ After the lamellar platelets were treated with ethanol (selective solvent for P2VP blocks) vapor for 1 h, the characteristic vibration associated with P2VP blocks could be clearly seen at 1589 cm^{-1} ($\nu(8b)$ of P2VP)⁵⁷ besides several characteristic vibrations associated with PS blocks (the top spectrum of Figure 3a). These results indicated that the surface of the lamellar platelets was mainly composed of the end PS blocks for lamellar platelets grown in toluene solution or treated with vapor of common solvent for PS and P2VP blocks. After being treated with the vapor of the selective solvent for P2VP blocks, the surface of the lamellar platelets partially contained the middle P2VP blocks. This conclusion could be further confirmed by AFM characterization.

Figure 4a shows the AFM height image of the upper surface of a typical platelet in the film spin-coated from toluene solution. The surface morphology was not quite smooth with a roughness of 0.98 nm although the phase separation was not obvious. Figure 4b shows the AFM height image of the upper surface of a typical platelet after treatment with 1,4-dioxane vapor for 60 min, which revealed a smooth, featureless surface with a roughness of 0.46 nm. The sample of Figure 4b was then further treated with toluene (Figure 4c) or ethanol (Figure 4d) vapor for 60 min. After the treatment in vapor of selective solvents, the roughness increased. Since toluene is the selective solvent

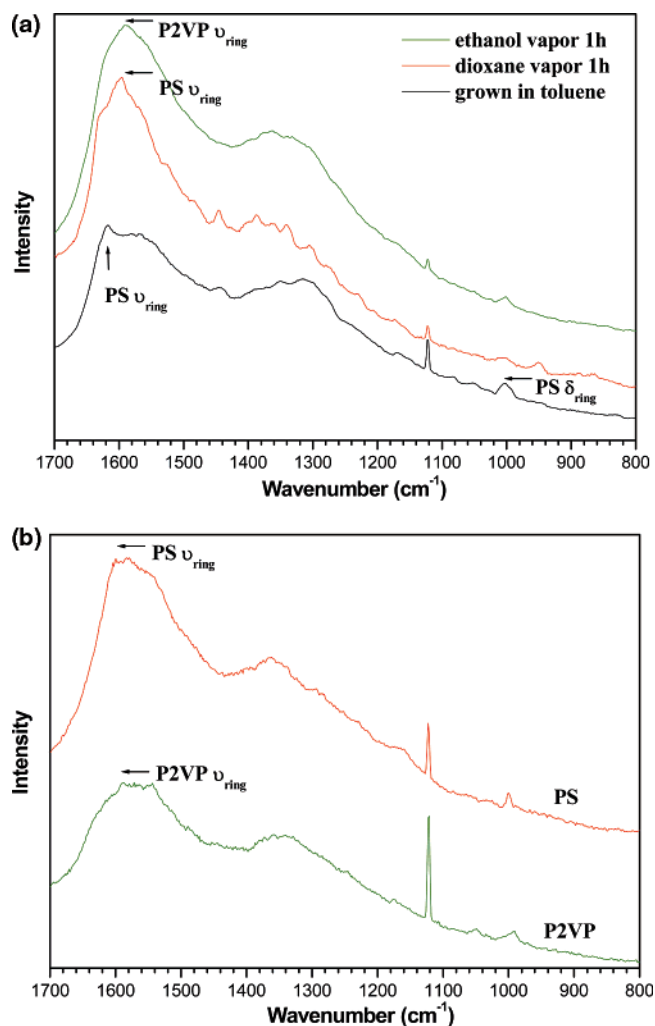


Figure 3. SERS spectra of 1# PS-*b*-P2VP-*b*-PEO lamellar platelets: (a) (bottom) spin-coated from toluene solution, (middle) after treatment in 1,4-dioxane vapor for 1 h, and (top) after treatment in ethanol vapor for 1 h; (b) SERS spectra of (bottom) homopolymer P2VP and (top) homopolymer PS.

for upper PS blocks, the change of the surface morphology is not obvious (Figure 4c, roughness from 0.46 to 0.55 nm). However, after treated in ethanol vapor (selective for lower P2VP blocks) for 60 min, an irregular wormlike network structure appeared on the surface with a roughness of 0.88 nm (Figure 4d). Figure 4e shows the AFM height image of the upper surface of a typical platelet after treated with ethanol vapor for 60 min from the original spin-coated platelets, which showed a similar surface pattern (roughness from 0.46 to 2.05 nm) with that successively treated by 1,4-dioxane and ethanol vapor (Figure 4d). The sample of Figure 4e was also further treated with toluene (Figure 4f) or 1,4-dioxane (Figure 4g) vapor for 60 min. The surface morphology after treated by ethanol and toluene vapor (Figure 4f, roughness of 0.51 nm) is similar to that after treated by 1,4-dioxane and toluene vapor (Figure 4c, roughness of 0.55 nm). On the other hand, the surface morphology after treated by ethanol and 1,4-dioxane vapor (Figure 4g, roughness 0.61 nm) is similar to that after solely treated by 1,4-dioxane vapor (Figure 4b, roughness 0.46 nm).

All these results revealed that surface morphologies were mainly determined by the last treatment process and the selectivity of tethered blocks to various solvent vapors is responsible for the different evolution of surface patterns on PEO platelets (Scheme 3). It has been found that tethered block

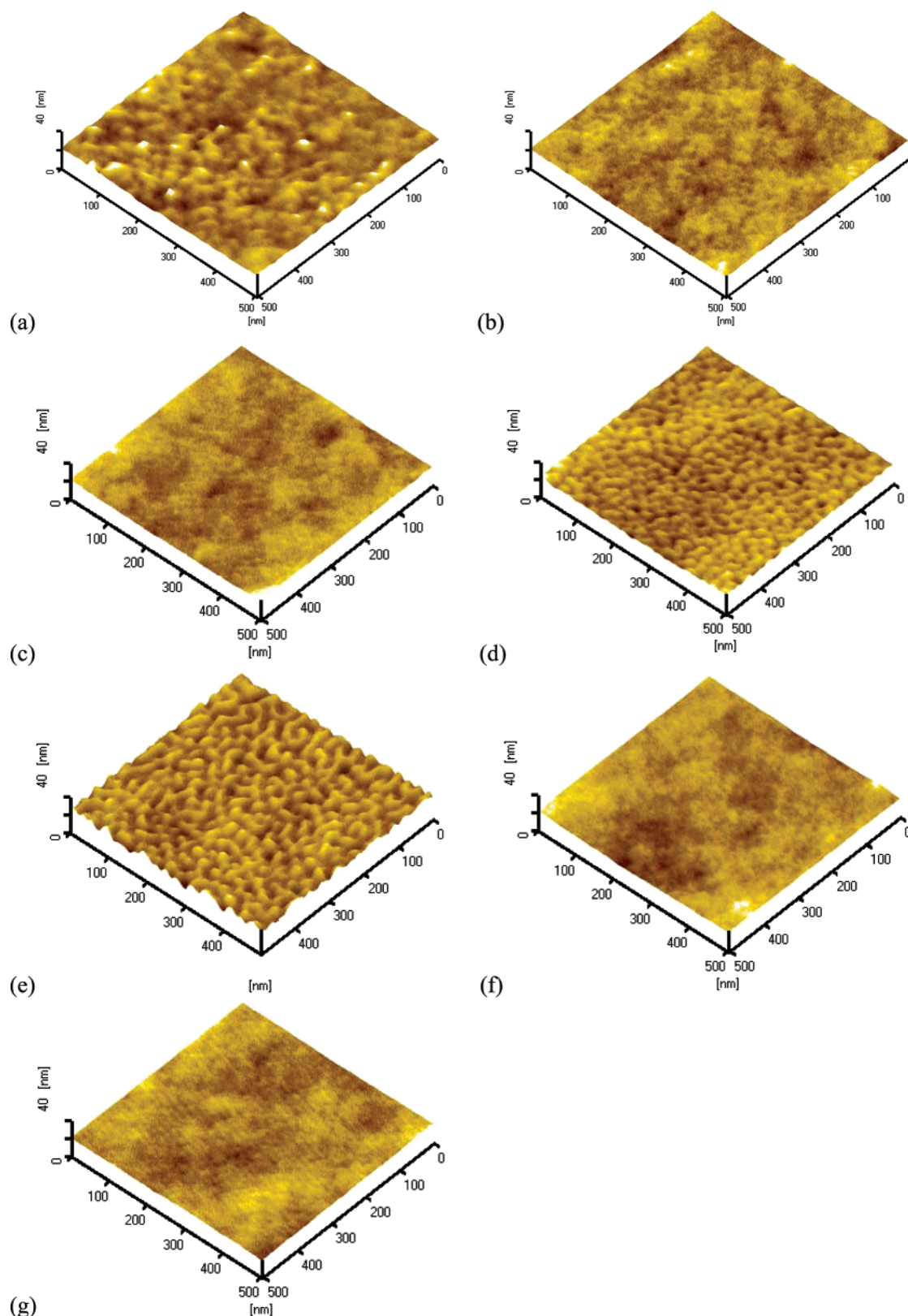
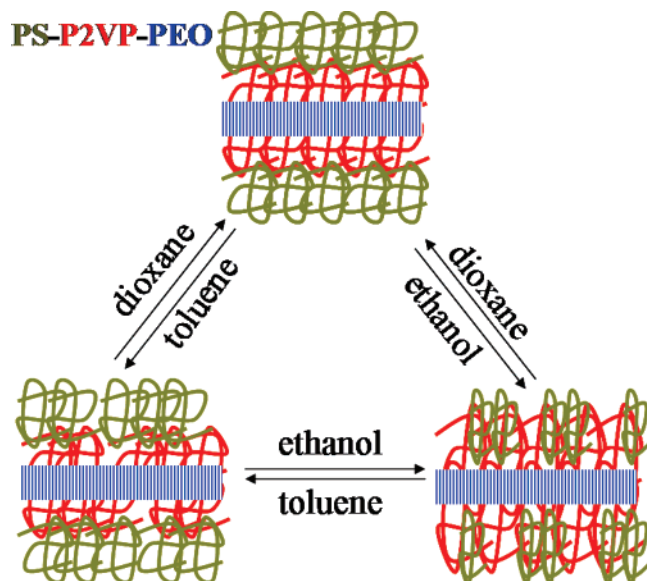


Figure 4. AFM height images of basal surfaces of PEO platelets (formed from 1# PS-*b*-P2VP-*b*-PEO 0.1 wt % in distilled toluene, $Z \approx 0-1.5$) before and after treated by different solvent vapor: (a) after spin-coating from toluene solution, (b) treated by 1,4-dioxane vapor for 60 min, (c) successively treated by 1,4-dioxane and toluene vapor for 60 min, (d) successively treated by 1,4-dioxane and ethanol vapor for 60 min, (e) treated by ethanol vapor for 60 min, (f) successively treated by ethanol and toluene vapor for 60 min, and (g) successively treated by ethanol and 1,4-dioxane vapor for 60 min.

copolymer chains self-assemble into micelles whose core is formed by less soluble blocks (the more soluble blocks form a shell around the core) in the selective solvents.^{7,58} When spin-coated from toluene solution (Figure 4a) or treated with toluene

vapor (Figures 4c and 3f), the morphology of the upper surface of platelets was not quite smooth (with roughness of 0.51–0.98 nm) and the phase separation was not obvious. Considering that toluene was a non-solvent for P2VP blocks and a good

Scheme 3. Schematic Representation of Changes of Surface Morphologies on the Basal Surface of Platelets with Response to Different Solvent Vapor



solvent for PS blocks, P2VP blocks adopted the collapsed conformation on the basal surface of PEO crystals and PS blocks adopted the conformation close to the random coil in the bulk (left part of Scheme 3).⁵⁹ After treated with ethanol vapor (Figures 4d and 3e), an irregular wormlike network structure appeared on the upper surface of the platelets (roughness of 0.88–2.05 nm). We speculate that P2VP blocks adopted random coil and PS blocks aggregated to form a core surrounded by P2VP blocks to avoid contact with ethanol vapor since ethanol was a selective solvent for P2VP blocks (right part of Scheme 3).⁷ After being treated with 1,4-dioxane vapor (Figure 4b, 3g), the morphology of the upper surface of platelets was smooth and featureless (with a roughness of 0.46–0.61 nm). This can be explained by the fact that 1,4-dioxane is the common solvent for P2VP and PS blocks and the phase separation in lateral direction cannot complete under the experimental conditions (upper part of Scheme 3).⁷

Conclusion

In summary, lamellar platelets were prepared in dilute toluene solution with trace amounts of water. In toluene solution the aggregation states of PS-*b*-P2VP-*b*-PEO were sensitive to the water content in the solution. For $Z \approx 1$, spherical micelles were formed in the early stage and large square platelets would gradually grow from these spherical micelles. The hydrogen bonding between water and EO units was responsible for the formation of micelles and subsequent square platelets in the solution. Tethered P2VP-*b*-PS chains on basal surface of PEO platelets could be regarded as diblock copolymer brushes and the density (σ : 0.086–0.36) and height (d : 3.5–14.3 nm) of these tethered chains could be easily modulated by changing the crystallization condition and/or the molecular weight of each block. The surface morphology of tethered P2VP-*b*-PS chains was responsive to different solvent vapors. The selectivity of tethered blocks to various solvents is responsible for the change of morphologies of the basal surface of the platelets. Our results confirm the leading role of water in the formation of reverse micelles and provide a convenient method to prepare and investigate tethered diblock copolymer chains with uniform and controllable chain tethering density and height.

Acknowledgment. This work is subsidized by the National Natural Science Foundation of China (Grants 20334010, 20621401, and 50573077).

References and Notes

- (1) Brittain, W. J.; Boyes, S. G.; Granville, A. M.; Baum, M.; Mirous, B. K.; Akgun, B.; Zhao, B.; Blickle, C.; Foster, M. D. *Adv. Polym. Sci.* **2006**, *198*, 125.
- (2) Zhulina, E. B.; Singh, C.; Balazs, A. C. *Macromolecules* **1996**, *29*, 6338.
- (3) Zhulina, E. B.; Singh, C.; Balazs, A. C. *Macromolecules* **1996**, *29*, 8904.
- (4) Dong, H.; Marko, J. F.; Witten, T. A. *Macromolecules* **1994**, *27*, 6428.
- (5) Yu, K.; Wang, H. F.; Xue, L. J.; Han, Y. C. *Langmuir* **2007**, *23*, 1443.
- (6) Xu, C.; Wu, T.; Drain, C. M.; Batteas, J. D.; Fasolka, M. J.; Beers, K. L. *Macromolecules* **2006**, *39*, 3359.
- (7) Zhao, B.; Brittain, W. J.; Zhou, W.; Cheng, S. Z. D. *Macromolecules* **2000**, *33*, 8821.
- (8) Mansky, P.; Liu, Y.; Huang, E.; Russell, T. P.; Hawker, C. J. *Science* **1997**, *275*, 1458.
- (9) Zhao, B.; Brittain, W. J. *Prog. Polym. Sci.* **2000**, *25*, 677.
- (10) Lin, E. K.; Gast, A. P. *Macromolecules* **1996**, *29*, 4432.
- (11) Chen, W. Y.; Li, C. Y.; Zheng, J. X.; Huang, P.; Zhu, L.; Ge, Q.; Quirk, R. P.; Lotz, B.; Deng, L.; Wu, C.; Thomas, E. L.; Cheng, S. Z. D. *Macromolecules* **2004**, *37*, 5292.
- (12) Chen, W. Y.; Zheng, J. X.; Cheng, S. Z. D.; Li, C. Y.; Huang, P.; Zhu, L.; Xiong, H.; Ge, Q.; Guo, Y.; Quirk, R. P.; Lotz, B.; Deng, L.; Wu, C.; Thomas, E. L. *Phys. Rev. Lett.* **2004**, *93*, 028301.
- (13) Zheng, J. X.; Xiong, H.; Chen, W. Y.; Lee, K.; Van Horn, R. M.; Quirk, R. P.; Lotz, B.; Thomas, E. L.; Shi, A.-C.; Cheng, S. Z. D. *Macromolecules* **2006**, *39*, 641.
- (14) (a) Xiong, H. M.; Zheng, J. X.; Cheng, S. Z. D.; Guo, Y.; Quirk, R. P.; Lotz, B. Single Crystal Engineering of Diblock Copolymer Brushes. Presented at APS March Meeting of the American Physical Society, Los Angeles, CA, 2005. (b) Xiong, H. M.; Zheng, J. X.; Van Horn, R. M.; Jeong, K.-U.; Quirk, R. P.; Lotz, B.; Thomas, E. L.; Brittain, W. J.; Cheng, S. Z. D. *Polymer* **2007**, *48*, 3732.
- (15) Li, B.; Li, C. Y. *J. Am. Chem. Soc.* **2007**, *129*, 12.
- (16) Lotz, B.; Kovacs, A. J. *Kolloid Z. Z. Polym.* **1966**, *209*, 97.
- (17) Lotz, B.; Kovacs, A. J.; Bassett, G. A.; Keller, A. *Kolloid Z. Z. Polym.* **1966**, *209*, 115.
- (18) Bassett, D. C. *Principles of Polymer Morphology*; Cambridge University Press: Cambridge, U.K., 1981.
- (19) Gohy, J.-F.; Willet, N.; Varshney, S.; Zhang, J.-X.; Jérôme, R. *Angew. Chem., Int. Ed.* **2001**, *40*, 3214.
- (20) Lei, L.; Gohy, J.-F.; Willet, N.; Zhang, J.-X.; Varshney, S.; Jérôme, R. *Macromolecules* **2004**, *37*, 1089.
- (21) Aizawa, M.; Buriak, J. M. *J. Am. Chem. Soc.* **2006**, *128*, 5877.
- (22) Bates, F. S.; Fredrickson, G. H. *Phys. Today* **1999**, *52*, 32.
- (23) Bang, J.; Kim, S. H.; Drockenmüller, E.; Misner, M. J.; Russell, T. P.; Hawker, C. J. *J. Am. Chem. Soc.* **2006**, *128*, 7622.
- (24) Pickett, G. T.; Balazs, A. C. *Macromol. Theory Simul.* **1998**, *7*, 249.
- (25) Huang, W. H.; Luo, C. X.; Zhang, J. L.; Han, Y. C. *J. Chem. Phys.* **2007**, *126*, 104901.
- (26) Kyritsis, A.; Pissis, P. *J. Polym. Sci., Part B: Polym. Phys.* **1997**, *35*, 1545.
- (27) Raviv, U.; Tadmor, R.; Klein, J. *J. Phys. Chem. B* **2001**, *105*, 8125.
- (28) Lei, L.; Gohy, J.-F.; Willet, N.; Zhang, J.-X.; Varshney, S.; Jérôme, R. *Polymer* **2006**, *47*, 2723.
- (29) Cogan, K. A.; Gast, A. P. *Macromolecules* **1990**, *23*, 745.
- (30) Vagberg, L. J. M.; Cogan, K. A.; Gast, A. P. *Macromolecules* **1991**, *24*, 1670.
- (31) Gast, A. P.; Vinson, P. K.; Cogan-Farinas, K. A. *Macromolecules* **1993**, *26*, 1774.
- (32) Wu, G.; Zhou, Z.; Chu, B. *Macromolecules* **1993**, *26*, 2117.
- (33) Wu, G.; Chu, B. *Macromolecules* **1994**, *27*, 1766.
- (34) Guo, C.; Liu, H. Z.; Chen, J. Y. *Colloids Surf. A* **2000**, *175*, 193.
- (35) Cosgrove, T. *Faraday Discuss.* **1994**, *98*, 231.
- (36) Bhargava, P.; Zheng, J. X.; Li, P.; Quirk, R. P.; Harris, F. W.; Cheng, S. Z. D. *Macromolecules* **2006**, *39*, 4880.
- (37) Bhargava, P.; Tu, Y.; Zheng, J. X.; Xiong, H.; Quirk, R. P.; Cheng, S. Z. D. *J. Am. Chem. Soc.* **2007**, *129*, 1113.
- (38) (a) Cao, L.; Manners, I.; Winnik, M. A. *Macromolecules* **2002**, *35*, 8258. (b) Gohy, J.-F.; Lohmeijer, B. G.; Alexeev, A.; Wang, X.-S.; Manners, I.; Winnik, M. A.; Schubert, U. S. *Chem.—Eur. J.* **2004**, *10*, 4315.
- (39) (a) Fujiwara, T.; Miyamoto, M.; Kimura, Y. *Macromolecules* **2000**, *33*, 2782. (b) Fujiwara, T.; Miyamoto, M.; Kimura, Y.; Sakurai, S. *Polymer* **2001**, *42*, 1515. (c) Fujiwara, T.; Miyamoto, M.; Kimura, Y.; Iwata, T.; Doi, Y. *Macromolecules* **2001**, *34*, 4043.
- (40) Liu, L.-Z.; Jiang, B. *J. Polym. Sci., Part B* **1998**, *36*, 2961.

- (41) Wolff, M.; Scholz, U.; Hock, R.; Magerl, A.; Leiner, V.; Zabel, H. *Phys. Rev. Lett.* **2004**, 92, 255501.
- (42) (a) Xu, J. T.; Jin, W.; Liang, G. D.; Fan, Z. Q. *Polymer* **2005**, 46, 1709. (b) Xu, J. T.; Fairclough, J. P. A.; Mai, S. M.; Ryan, A. J. *J. Mater. Chem.* **2003**, 13, 2740.
- (43) Ræz, J.; Tomba, J. P.; Manners, I.; Winnik, M. A. *J. Am. Chem. Soc.* **2003**, 125, 9546.
- (44) Zhang, J.; Wang, J.-Q.; Wang, H.; Tu, K. *Biomacromolecules* **2006**, 7, 2492.
- (45) Xu, J. T.; Fairclough, J. P. A.; Mai, S. M.; Ryan, A. J. *J. Mater. Chem.* **2003**, 13, 2740.
- (46) Huang, W. H.; Luo, C. X.; Li, B. Y.; Han, Y. C. *Macromolecules* **2006**, 39, 8075.
- (47) Sasaki, T.; Miyazaki, A.; Sugiura, S.; Okada, K. *Polym. J.* **2002**, 34, 794.
- (48) Riess, G. *Prog. Polym. Sci.* **2003**, 28, 1107.
- (49) Gervais, M.; Gallot, B. *Makromol. Chem.* **1977**, 178, 2071.
- (50) Kovacs, A. J.; Manson, J. A. *Kolloid Z. Z. Polym.* **1966**, 214, 1.
- (51) Reiter, G.; Hoerner, P.; Hurtrez, G.; Riess, G.; Sommer, J. U.; Joanny, J. F. *J. Surf. Sci. Technol.* **1998**, 14, 93.
- (52) Hamley, I. W. *Adv. Polym. Sci.* **1999**, 148, 113.
- (53) Skoulios, A. E.; Tsouladze, G.; Franta, E. *J. Polym. Sci. C* **1963**, 4, 507.
- (54) Gervais, M.; Gallot, B. *Makromol. Chem.* **1973**, 171, 157.
- (55) Gervais, M.; Gallot, B. *Makromol. Chem.* **1973**, 174, 193.
- (56) (a) Ding, N.; Amis, E. J.; Yang, M.; Salovey, R. *Polymer* **1988**, 29, 2121. (b) Ding, N.; Amis, E. J. *Macromolecules* **1991**, 24, 3906.
- (57) Tsai, W. H.; Boerio, F. J.; Clarson, S. J.; Parsonage, E. E.; Tirrell, M. *Macromolecules* **1991**, 24, 2538.
- (58) Zhulina, E. B.; Singh, C.; Balazs, A. C. *Macromolecules* **1996**, 29, 8254.
- (59) Spatz, J. P.; Sheiko, S. S.; Möller, M. *Adv. Mater.* **1996**, 8, 513.

MA070926S